GEOMETRIC VALIDATION OF CARTOSAT-1 IMAGERY

S. Kocaman [*], K. Wolff, A. Gruen, E. Baltsavias

Institute of Geodesy and Photogrammetry, ETH Zurich
Wolfgang-Pauli-Str. 15, CH-8093 Zurich, Switzerland – (skocaman, wolff, agruen, manos@geod.baug.ethz.ch)

Commission I, SS-11

KEY WORDS: Satellite Remote Sensing, Digital Surface Models (DSM), Image Matching, Adjustment, Topographic Mapping, Image Processing, Accuracy Analysis

ABSTRACT:

The Institute of Geodesy and Photogrammetry (IGP) is participating in the Cartosat-1 evaluation program, a common initiative of ISRO (India) and ISPRS. Within this program, various test sites with reference data have been established and Cartosat-1 images have been acquired over these sites. We have reported already about the Rome and Mausanne datasets in a former publication. Here, we report about our investigations at the Catalonia test site of ISRO. In addition, we evaluate the Cartosat-1 images acquired over the test site in Sakurajima, Japan. First, we report on image preprocessing for their improvement. Then, we report on RPC refinement and the 3D point positioning accuracy that can be achieved with the Rational Polynomial Coefficients (RPCs) sensor model. The orientation results include various options regarding sensor model and number and distribution of GCPs. The best results led to planimetric and height accuracies (RMSE) of about half a ground pixel size (2.5m) in both planimetry and height. Finally, we present the results of automatic DSM generation using our own SAT-PP program package. The results were checked both visually and were compared using the provided reference data (Catalonia DTM and Sakurajima DSM). While for the Catalonia test site the achieved height accuracy is about 3 m (sigma), confirming previous results we have reported in other test sites, for Sakurajima the results are significantly worse mainly due to the terrain relief.

1. INTRODUCTION

High spatial resolution optical satellite sensors have been subject of scientific investigations and evaluations since 2000. Some of them provide a ground sampling distance (GSD) of 1m or less but each image covers a small area, their price is high, and stereo coverage is often rare. Thus, the last years some sensors have been launched with a GSD of 2.5 – 5 m, covering a much larger area per image, having much lower image price and tailored to acquisition of stereo images and derivation of DSMs by using 2- or 3-Linear Array CCD sensors. Typical examples include Spot-5 HRG, ALOS/PRISM and Cartosat-1. Such systems are suitable also for derivation of global DSMs, if the absolute geolocation accuracy of the images is good enough (e.g. SPOT-5, ALOS/PRISM).

A description of the Cartosat-1 mission is given in Krishnaswamy and Kalyanaraman (2002), Krishnaswamy (2002), Cartosat-1 Handbook (2006), EOPortal (2007) and Cartosat (2008). Here, we remind some of the parameters, which are relevant for the discussion below. Cartosat-1 has a fore (F) and aft (A) panchromatic camera for along-track stereo, with a tilt in flight direction of +26° and -5°, respectively. Each sensor is comprised of 12,000 pixel CCDs with 7 microns pixel spacing. Each sensor uses two staggered lines, which take images with a time difference of about 1.7 ms (the distance between the two lines in flight direction is 35 microns). The aim of the staggering is not the increase of spatial resolution (only odd and even pixels are read-out) but a faster read-out, permitting the integration time needed in order to achieve a pixel footprint of 2.2-2.5 m in flight direction. The CCDs, identical to the one of Cartosat-2, are not of TDI (Time Delay

and Integration) technology and the integration time is 0.366 ms, so rather short compared to the usual target value of 1-2 ms. The nominal base to height (B/H) ratio is 0.62. Data are quantized with 10-bit and compressed by a factor of 3.22, with little image quality loss. The nominal GSD is 2.2-2.5m, and the typical image size is 12,000 x 12,000 pixels. The image scale is about 1:312,000. The geolocation accuracy of the images, as given by ISRO, (without GCPs, 3-sigma) is 250 m (design) and 150 m (achieved). The satellite has a yaw steering, in order to compensate the Earth rotation effect or to acquire a wider mono strip. A pitch bias (e.g. 5 deg, -21 deg, -10.5 deg) is also possible to acquire occluded areas in case of large slopes along track. A roll of the satellite body allows across-track pointing up to 23 degrees, increasing thus the revisit frequency. Dynamic changes, especially the continuous yaw steering and pitch bias (if applied during imaging) may affect both geometric stability and radiometric quality (image smearing).

A set of algorithms for processing of high resolution satellite imagery (HRSI) has been developed at the Institute of Geodesy and Photogrammetry (IGP), ETH Zurich and realized in a software suite called SAT-PP (Satellite Image Precision Processing). The SAT-PP features mainly include: GCP measurements, image georeferencing with RPC approach and various other sensor models, DSM generation with advanced multi-image geometrically constrained matching for linear array and frame sensors, ortho-image generation, and feature extraction. The software has been used for processing of a number of high resolution satellite sensors, such as IKONOS, QuickBird, ALOS/PRISM, and SPOT-5 HRS/HRG. Detailed information on the SAT-PP features can be found in Gruen et al. (2005).

---

[*] Corresponding author.

Our investigations on Cartosat-1 data focus on: a) radiometric problems and preprocessing for image quality improvement, b) RPC refinement and 3D point measurement accuracy potential, and c) automatic DSM generation. The SAT-PP functions are used for RPC refinement, and DSM generation in this study. The sensor modeling is performed via Rational Polynomial Coefficients (RPCs). Two different models are applied to improve the given RPCs by using ground control points (GCPs). The RPC correction models include two translational parameters (RPC1) and 2D affine transformation (RPC2). Different numbers and distribution of GCPs are used for the investigations.

The investigations in this paper are part of the ISPRS-ISRO Cartosat-1 Scientific Assessment Programme (C-SAP). IGP acts as principal investigator for some test sites and has evaluated data from other test sites. We have already reported on our investigations with the Rome and Mausanne test sites in Baltsavias et al. (2007). In this paper, we report on our investigations in the Catalonia test site (official C-SAP test site 10), Spain, and Sakurajima test site, Japan. Other results regarding the Catalonia test site are reported in Lehner et al. (2007).

2. INPUT DATA

A Cartosat-1 stereo pair acquired over the *Catalonia* test site is provided by ISRO within C-SAP (Test site 10). The GCP image coordinates are measured at the DLR, Germany, using the Least Squares Matching (LSM) method (Lehner et al., 2007). Some details on the dataset are given in Table 1. The GCP distribution over the Cartosat-1 Aft image can be seen in Figure 1. As reference data, a DTM with a 15 m grid spacing and orthoimages with scale 1:5000 were provided by the Institut Cartogràfic de Catalunya (ICC), Spain for the whole testfield. The date of primary data acquisition for the DTM is unknown; this can result in differences in the comparison with the Cartosat matching DSM due to temporal differences.
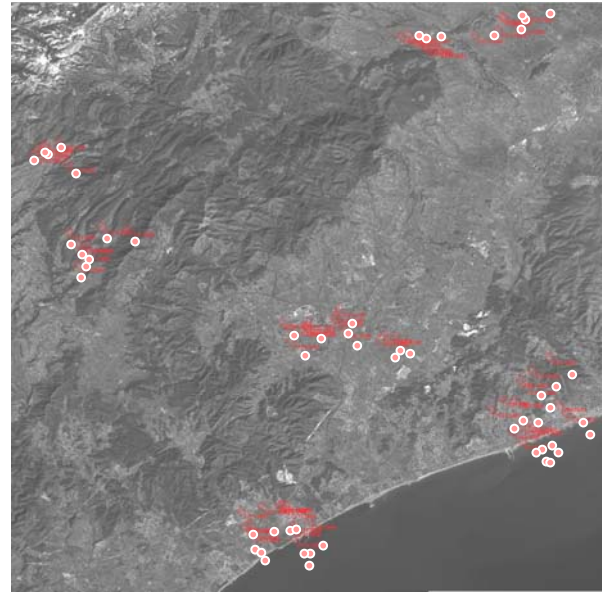

Figure 1. GCP distribution over the Cartosat-1 Aft image of the Catalonia test site

Figure 2. GCP distribution over the Cartosat-1 Aft image of the Sakurajima test site

Imaging date	01 Feb 2006	
Sun Azimuth	Aft: 157.16918°	Fore: 158.65601°
Sun Elevation	Aft: 31.65443°	Fore: 28.91865°
No. of GCPs	70	
Point measurement method	69 points are measured with LSM and 1 point is measured manually	
Reference DTM	29 km x 25 km	
- grid spacing	15 m	
- accuracy (1σ)	1.1 m	
- height range	0 m – 970 m	

Table 1. Catalonia Cartosat-1 test dataset description.

The *Sakurajima* testfield is generated as a joint project of the Kochi Institute of Technology and Kanazawa Institute of Technology. 62 GCPs are provided by the Japan Association of Remote Sensing (JARS) and 61 points could be measured on the Cartosat-1 images (Figure 2). However, just a small area about 4 km to 4 km of the volcano Sakurajima is given as a 5m grid laser scanner reference dataset provided by Kokusai Kogyo Co. Ltd, Japan (see Figure 7). Main characteristics of the test site and the Cartosat-1 stereo pair are given in Table 2. ALOS/PRISM images acquired over the same test site are processed and the results are reported in Gruen et al. (2008).

Imaging date	31 March 2006	
Sun Azimuth	Aft: 139.17555°	Fore: 143.38021°
Sun Elevation	Aft: 59.43782°	Fore: 57.26630°
No. of GCPs	61	
Point measurement method	58 points are measured with LSM and 3 points are measured manually	
Reference DSM	4 km x 4 km	
- method	laser scanning	
- grid spacing	5 m	
- height range	300 m – 1100 m	
- remark	no GCP inside reference DSM	

Table 2. Sakurajima Cartosat-1 test dataset description
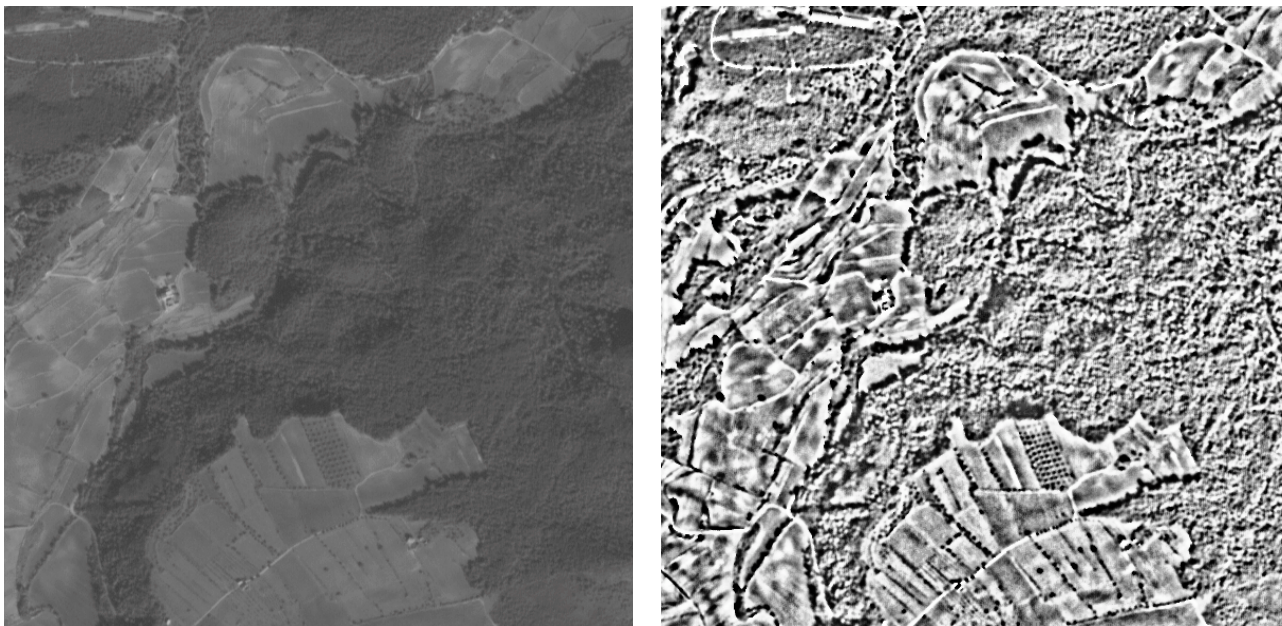
Figure 3. Catalonia image. Left original, right after preprocessing.

3. IMAGE QUALITY AND PREPROCESSING

In Baltsavias et al. (2007), we have reported about image quality. The images in this test, which are later than the images commented in the previous investigations, are generally better. Pattern noise is less and the edge jitter of horizontal edges is almost invisible. The interlacing noise still remains, and the Fore channel images compared to the Aft ones are less sharp, partly to the different ground pixel resolution.

The preprocessing performed was applied to the original 10-bit images, along the same line as mentioned in Baltsavias et al. (2007). First, an adaptive noise filtering was applied to reduce noise without smoothing edges, then Wallis filtering to enhance contrast, especially in dark regions, and to radiometrically equalize the images used for matching. Finally, the images were reduced to 8-bit for further processing, since many software packages for matching including our SAT-PP (see Section 5) can not handle images with more than 8-bit. An example of preprocessing is shown in Figure 3.

4. SENSOR ORIENTATION AND ACCURACY OF 3D POINT MEASUREMENT

Sensor orientation is performed using RPCs provided by ISRO. We have applied correction to the RPCs by two shifts (RPC1) and by an affine transformation (RPC2). Six and all GCP versions are tested in both models. For the 6 GCP case, we have applied two different distributions by covering the whole and $1/4^{th}$ of the image area. The results are reported in Table 3 and Table 4 for both datasets.

The estimated line and sample shift values in Catalonia dataset are approximately (49, -34) and (51, -14) pixels for the aft and fore images, respectively. For the Sakurajima dataset, shift corrections are approximately (-87, -41) and (-104, -8) pixels in the line and sample directions of the aft and fore images, respectively. The values are obtained from the RPC2 method using all GCPs. These values give an indication of absolute geolocation accuracy of Cartosat-1.

Method	GCP no	RMSE X (m)	RMSE Y (m)	RMSE Z (m)	$Sigma_0$ (pixel)
RPC-1	All (70)	2.12	1.84	4.23	1.07
RPC-1	6 *	2.15	2.01	4.25	0.78
RPC-1	6 **	2.12	2.04	4.53	0.32
RPC-2	All (70)	0.94	1.31	1.26	0.50
RPC-2	6 *	0.98	1.43	1.49	0.41
RPC-2	6 **	1.23	2.02	1.60	0.21

* GCPs well-distributed over the images.
** GCPs cover approximately $1/4^{th}$ of the image area.

Table 3. Triangulation results of the Catalonia dataset.

Method	GCP no	RMSE X (m)	RMSE Y (m)	RMSE Z (m)	$Sigma_0$ (pixel)
RPC-1	All (61)	1.90	3.42	5.02	1.46
RPC-1	6 *	1.97	3.47	5.27	0.95
RPC-1	6 **	2.00	3.95	5.77	0.65
RPC-2	All (61)	1.43	1.31	1.42	0.62
RPC-2	6 *	1.64	1.55	1.77	0.40
RPC-2	6 **	2.73	2.50	2.10	0.41

* GCPs well-distributed over the images.
** GCPs cover approximately $1/4^{th}$ of the image area.

Table 4. Triangulation results of the Sakurajima dataset.

In both datasets, the RMSE values for RPC2 are at sub-pixel level. The accuracy, for both RPC1 and especially RPC2, which is necessary for higher accuracy, deteriorates with poor GCP distribution. The RPC1 method (only shift correction) gives much inferior results compared to RPC2, especially in height. For the DSM generation, the RPC2 and all GCPs versions have been used.

5. DSM GENERATION AND ACCURACY ANALYSIS

The image matching process was realized by using the program package SAT-PP developed at IGP, which has been used extensively for various platforms, sensors and image scales with very good results, published for several projects. More details about the underlying algorithm can be found in Zhang (2005).

SAT-PP produced very densely matches. It is using multiple match-point primitives (regular image grid points, interest points and edgels). For both test areas, we chose a modified cross-correlation matching and no LSM at the final stage.

A quantitative 3D evaluation was realized by co-registering the generated DSM and the reference DSM/DTM by using the method described in Gruen and Akca (2005). With the respective program LS3D, three shift parameters (Tx, Ty and Tz) were determined between the two dataset to remove possible offsets. After this co-registration, the Euclidian distances (E) between the two DSMs are computed point-wise, and the error is also split into its X, Y and Z components.

5.1 Testfield Catalonia

For the whole area, a DTM with a grid size of 15 m was provided. For the generated DSM, we chose a grid size of 10 m, corresponding to 4 times the GSD of Cartosat-1. About half of the testfield is a hilly region with forest, trees and bushes and open area. The rest is a flat area with a part of the city of Barcelona, some villages, trees and open areas. A lake and the sea were excluded from the evaluation (see Figure 4).
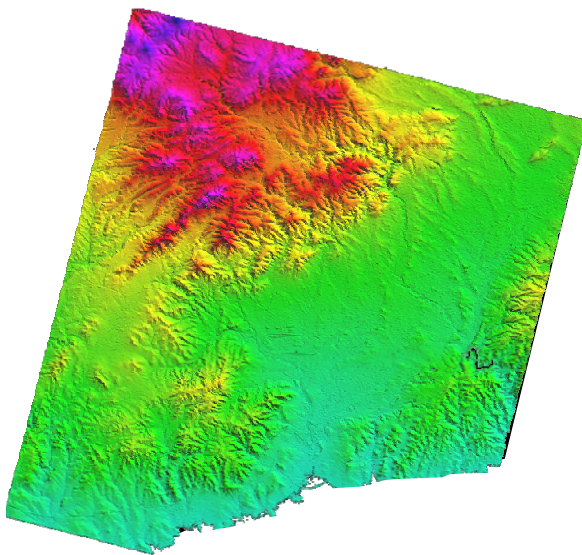

Figure 4. Generated DSM of the testfield Catalonia (grid spacing 10m). The black area is an excluded lake area. The size of the evaluation area is 29 km x 25 km.

The results of the 3D evaluation are summarized in Table 5 and visualized in Figure 5. The residuals smaller than -3 sigma and larger than +3 sigma are very few. The larger errors are mainly caused by shadow areas and differences between the reference DTM and the matching DSM, like trees (see reddish areas in Figure 5) and multitemporal differences, like surface mining (see white circles in Figure 5), while the bluish arc at the bottom left is due to a highway.
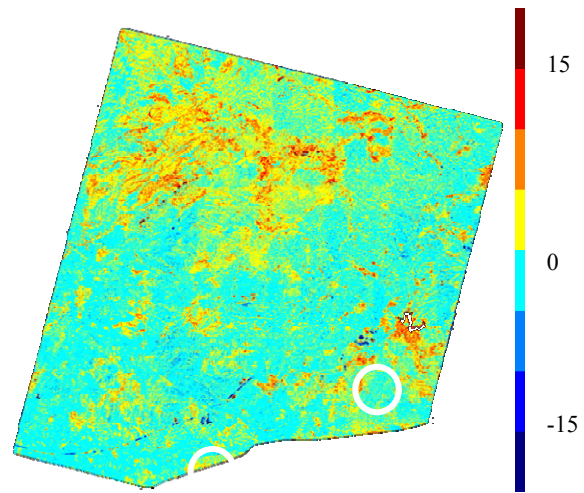

Figure 5. Color coded image of the Euclidian distances (DSM – reference). The color intervals correspond to 5m. The two white circles show the blunders caused by surface mining.

5.2 Testfield Sakurajima

The main characteristics of the steep volcanic area results in the following matching conditions: a large part of the area of interest was covered by shadows, clouds obscure a part of the image, the texture is generally weak, while the perspective differences at steep slopes were very large (see Figure 6).
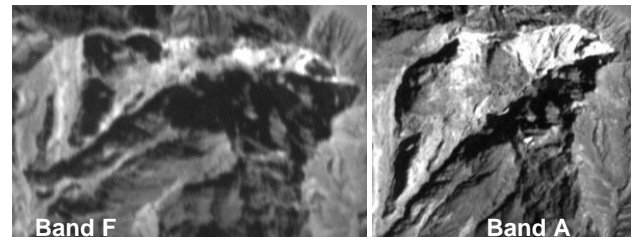

Figure 6. Blunder area resulting from different viewing angles causing large perspective differences at terrain with large slope and unfavorable aspect (see also Figure 8).
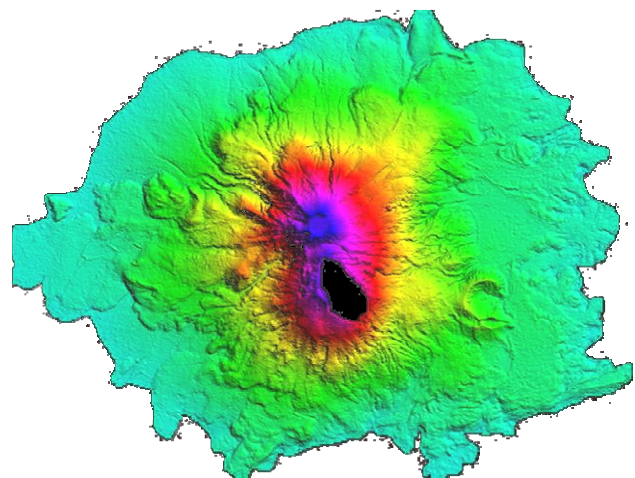

Figure 7. Generated DSM of the volcano Sakurajima, grid spacing 5m. The central red/blue part corresponds approximately to the DSM evaluation area (4km x 4km). The black area is excluded because of clouds in the images

Dataset	No. of used points	RMSE-E (m) RMSE-X (m) RMSE-Y (m) RMSE-Z (m)	Mean / Min / Max – E (m) Mean / Min / Max – X (m) Mean / Min / Max – Y (m) Mean / Min / Max – Z (m)	Tx / Ty / Tz (m)
Catalonia, DTM	2870270	3.14 0.62 0.75 2.98	0.02 / -56 / 63 0.00 / -40 / 28 0.01 / -35 / 60 0.00 / -51 / 55	1.33 / -3.61 / -1.16
Sakurajima, DSM	394962	9.26 4.68 3.77 7.04	1.00 / -160/ 153 -0.14 / -66 / 156 -0.11 / -65 / 51 0.61 / -66 / 135	1.41 / -2.63 / -1.09

Table 5. Statistical values of the Euclidean distance (E) differences between reference DSM (in Sakurajima) and DTM (in Catalonia) and matching DSM and values of the shift parameters (T) between the reference data and the Cartosat-1 DSM.
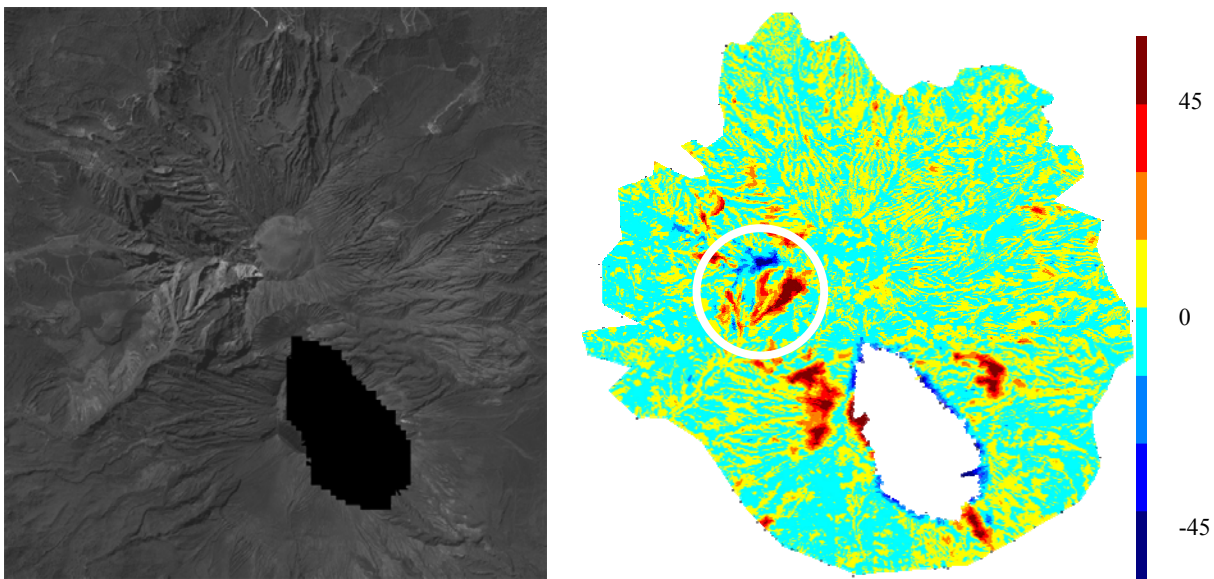

Figure 8. Left: Orthophoto of the area used for the evaluation of the DSM generation with reference data. The black area is the excluded cloud area. Right: Colour coded image of the Euclidian distances (DSM – reference). The color intervals correspond to 15 m. The white circle defines a critical area shown in detail in Figure 6. The other reddish areas around the cloud area are also due to shadows and mainly very large perspective differences.

A color coded and shaded view of the generated DSM is presented in Figure 7. Figure 8 shows an orthophoto of the area with the typical structure of a volcano and the large shadow areas. One of the two calderas had to be excluded because of occlusion by clouds.

The results of the Cartosat-1 DSM valuation are summarized in Table 5 and visualized in Figure 8. The big blunders and the resulting worse accuracy are partly due to the steep volcano surface with terrain cuts, partly also having shadows and/or causing occlusions, low texture and large perspective differences. Additionally, there are also blunders around the excluded cloud area (see Figure 8). The larger sigma X and Y values in Table 5, compared to the Catalonia dataset, are due to the mountain slopes, with inclined Euclidean distance errors projected more in planimetry.

6. CONCLUSIONS

Regarding image quality, these Cartosat-1 images were better than other ones used in previous tests. The major remaining problems are the interlacing noise and the blurring of the Fore channel.

Regarding the necessary RPC refinement and the accuracy potential for 3D point measurement, the following can be concluded. RPCs should be corrected by an affine transformation, shifts alone do not suffice. The shifts with or without affine terms were much smaller than in previous tests, showing an improved absolute geolocation accuracy. The GCP distribution, although for many high resolution satellite sensors (e.g. Ikonos), is not so important, for Cartosat-1 seems to have an influence on the accuracy, especially in the planimetry. Thus, to be on the safe side, a good GCP distribution is recommended. The number of the GCPs is not so crucial. For an affine correction of the RPCs and a certain redundancy, we recommend the use of about 6 GCPs as minimum. Despite the suboptimal B/H ratio, the height accuracy in pixels was exceptionally good, even exceeding previous results achieved with sensors like IKONOS. This indicates that the errors in the planimetric positioning are rather due to the poor identification of the GCPs.

The DSM accuracy in Catalonia was slightly more than one pixel, without any manual editing, and in spite of multitemporal differences with the reference data, which was a DTM. For Sakurajima, the DSM results were poorer, mainly due to the reasons explained in Section 5.2. Thus, these results are not representative of the Cartosat-1 potential. In general, Cartosat-1 has a good potential for generation of DSMs with a grid spacing of about 10 m and accuracy (RMSE) of about 3 m. However, this can be achieved only by using GCPs (modest in number, but well measurable).

ACKNOWLEDGEMENTS

REFERENCES

Baltsavias, E., Kocaman, S., Akca, D., Wolff, K., 2007. Geometric and radiometric investigations of Cartosat-1 data. In: International Archives of Photogrammetry, Remote Sensing and Spatial Information Sciences, 36(1/W51), 13 p., on CD-ROM. Available at http://www.commission1.isprs.org/hannover07/start.htm (accessed 29 January, 2008).

Cartosat, 2008. http://www.isro.org/Cartosat/ (accessed 29 January, 2008).

Cartosat-1 Handbook, 2006. Available at http://www.nrsa.gov.in/IRS_Documents/Handbook/cartosat1.pdf (accessed 29 January, 2008).

EOPortal, 2007. http://directory.eoportal.org/pres_IRSP5IndianRemoteSensingSatelliteP5CartoSat1.html (accessed 29 January, 2008).

Gruen, A., Akca, D., 2005. Least squares 3D surface and curve matching. ISPRS Journal of Photogrammetry and Remote Sensing, 59(3), pp. 151-174.

Gruen A., Zhang L., Eisenbeiss H., 2005. 3D Precision Processing Of High Resolution Satellite Imagery. ASPRS 2005, Baltimore, Maryland, USA, March 7-11 (on CD-ROM).

Gruen, A., Murai, S., Baltsavias, E., Kocaman, S., Wolff, K., Hanusch, T., 2008. Investigations on the ALOS/PRISM and AVNIR-2 Sensor Models and Products. Interim PI Report for JAXA, 31 January.

Krishnaswamy, M., 2002. Sensors and Platforms for High Resolution Imaging for Large Scale Mapping Applications - Indian Scenario. Indian Cartographer, DAPI-01, URL: http://www.incaindia.org/technicalpapers/02_DAPI01.pdf (accessed 29 January, 2008).

Krishnaswamy, M., Kalyanaraman, S., 2002. Indian Remote Sensing Satellite Cartosat-1: Technical features and data products. Paper presented at Map Asia 2002 conference, 7-9 August, Bangkok, Thailand. Available at http://www.gisdevelopment.net/technology/rs/techrs023.htm (accessed 29 January, 2008).

Lehner, M., Müller, R., Reinartz, P., Schroeder, M., 2007. Stereo Evaluation of CARTOSAT-1 Data for French and Catalonian Test Sites. In: International Archives of Photogrammetry, Remote Sensing and Spatial Information Sciences, 36(1/W51), 5 p., on CD-ROM. Available at http://www.commission1.isprs.org/hannover07/start.htm (accessed 29 January, 2008).

Zhang, L., 2005. Automatic Digital Surface Model (DSM) Generation from Linear Array Images. Ph.D. Dissertation, Report No. 88, Institute of Geodesy and Photogrammetry, ETH Zurich. Available at http://e-collection.ethbib.ethz.ch/ecol-pool/diss/fulltext/eth16078.pdf (accessed 29 January, 2008